

RESEARCH ARTICLE

Advanced Bioprinting Methodologies: A Quantitative Analysis and Exploration of Innovative Techniques for Tissue Engineering

Reza Barbaz-Isfahani^{1*}, Amirhosein Shahbaz², Mahsa Jamali³, Abbasali Khademi⁴, Foad Iranmanesh⁵, Pedram Iranmanesh⁴, Amirshalar Khandan^{4**}, Erfan Sheikhbahaei⁶

¹ Department of Mechanical Engineering, University of Isfahan, Isfahan, Iran

² Department of Materials Engineering, Karaj Branch, Islamic Azad University, Karaj, Iran

³ Faculty of Mathematics, Statistics and Computer Science, University of Tabriz, Tabriz, Iran

⁴ Department of Endodontics, Dental Research Center, Dental Research Institute, School of Dentistry, Isfahan University of Medical Sciences, Isfahan, Iran

⁵ Department of Endodontic, School of Dentistry, Rafsanjan University of Medical Sciences, Rafsanjan, Iran

⁶ Medical Doctor, Independent Researcher, Toronto, Ontario, M2M 2T6, Canada

ARTICLE INFO

Article History:

Received 25 Oct 2024

Accepted 16 Jan 2025

Published 01 Mar 2025

Keywords:

3D Bioprinting

Hydrogels

Biological Inks

Crosslinking

Tissue Engineering

Additive Manufacturing

ABSTRACT

3D printing, also known as additive manufacturing, is an emerging technology with significant applications across various industries, including biomedical engineering. This study shows the diverse methods of 3D bioprinting and their capabilities. The fundamental components of 3D printing, including printers, inks, and software, are discussed, highlighting the importance of geometric infill. The study then delves into the three main bioprinting technologies: laser-based, extrusion, and inkjet printing, each with its unique strengths and weaknesses. The article emphasizes the crucial role of biological inks, or bioinks, in achieving the desired mechanical, chemical, and morphological properties of printed tissues and organs. Hydrogels, in particular, are highlighted as promising bioinks due to their biocompatibility, swelling properties, and ability to be modified for specific applications. The study examines both physical and chemical gelation mechanisms, discussing the advantages and limitations of each approach. The significance of crosslinking, whether achieved via photo crosslinking or chemical crosslinkers, is highlighted due to its vital role in preserving the structural integrity and mechanical properties of printed constructs. Furthermore, hybrid hydrogel development, comprising synthetic and natural polymers, is investigated as a strategy to synergistically combine the advantageous properties of both material classes. This study concludes by showing the significant progress made in the field of 3D bioprinting, while acknowledging the ongoing challenges in fully replicating the complexity of natural tissues and organs. The study shows the need for continued research and development to advance this technology and its applications in the biomedical field.

How to cite this article

Barbaz-Isfahani R., Shahbaz A., Jamali M., Khademi A., Iranmanesh F., Iranmanesh P., Khandan A., Erfan Sheikhbahaei. Advanced Bioprinting Methodologies: A Quantitative Analysis and Exploration of Innovative Techniques for Tissue Engineering. *Nanomed Res J*, 2024; 10(1): 95-113. DOI: 10.22034/nmrj.2025.01.010

INTRODUCTION

Three-dimensional (3D) printing, alternatively termed additive manufacturing, constructs objects via layer-by-layer material deposition [1-5]. This defining technology of the third industrial revolution integrates digital modeling,

electromechanical deposition systems, materials science, and chemical processing within an informatics framework [6-11]. Table 1 provides a consolidated overview of the core advantages and limitations inherent to 3D printing technologies within biomedical applications, highlighting both transformative capabilities, including cost efficiency, accelerated production, design versatility, and enhanced quality control, and persistent

* Corresponding Author Email: R.barbaz@eng.ui.ac.ir
sas.khandan@iaukhsh.ac.ir

challenges such as intrinsic speed constraints in layer deposition and the unresolved complexity of vascular network fabrication for volumetric tissues. Moreover, different methods of comparative analysis for the construction of the structure are also given in the Table 2 [12]. The printable forms of materials vary depending on different machines and can be in the form of powder, filament, or liquid, allowing them to be arranged into desired three-dimensional patterns. The technology of 3D printing was commercialized for the first time by Charles Hull [13].

Today, due to its flexibility, this technology is gaining attention as a comprehensive tool in various fields including bioprosthetic reconstruction, jewelry making, structural design, electronics, food industries, and aerospace-related products. In the

automotive and aerospace industries, lightweight 3D-printed parts with complex and advanced geometries reduce material consumption, costs, and time. In construction, this technology can be utilized from initial prototype design to demolition, as well as printing parts of buildings or entire structures, accelerating construction processes [14]. In the past, 3D printing has been extensively used for designing electronic devices, sensor electrodes, adaptive designs through the incorporation of conductive agents, and other practical applications. In this regard, thermoplastics, ceramics, graphene-based conductive materials, aerogels, hydrogels, and metals are among the materials that can now be printed using this technology. Research is ongoing in the use of novel materials, creating desirable properties, and overcoming existing limitations

Table 1. Advantages and Limitations of 3D Printing in Biomedical Applications

Aspect	Details	Category
Cost Reduction	Reduced material waste and streamlined production workflows.	Advantage
Production Speed	Faster prototyping compared to traditional manufacturing.	Advantage
Design Flexibility	Enables complex geometries (e.g., patient-specific implants).	Advantage
Quality Control	In-process monitoring improves product consistency.	Advantage
Printing Speed	Limited by layer-by-layer deposition; scalability challenges for large organs.	Limitation
Vascularization	Difficulty in fabricating functional vascular networks for thick tissues.	Limitation

Table 2. Different methods of comparative analysis for structure construction

Technique	Disadvantages	Advantages
Conventional bulk materials	Simple Large scale production	Larger layer thickness (~100 μm)
Freeze casting	Controlled interface behavior with variety of materials, bulk materials production with high toughness, controlled thickness	Mineral volume fractions are not equivalent to nacre composition Difficult control the segmented overlap minerals
Layer-by-layer deposition	Controlled thickness with nano dimension, comparative loading of mineral phase, ability to fabricate homogeneous film	Time consuming method Scaling is difficult reduced mechanical properties at higher concentration
Self-assembly	Possibility of molecular level assembly, bulk layer materials	Difficult to scaled fabrication
Self-assembly 3D printing	Rapid production, printing of complex structure, on demand printing, possibility of structural customization, Ability to print various biological inspired architecture with higher mineral concentration, utilized as efficient predictive tool for improved synthetic materials	Printing of limited number of materials, inability to combine nanoscale printing with macroscale design Control over surface quality

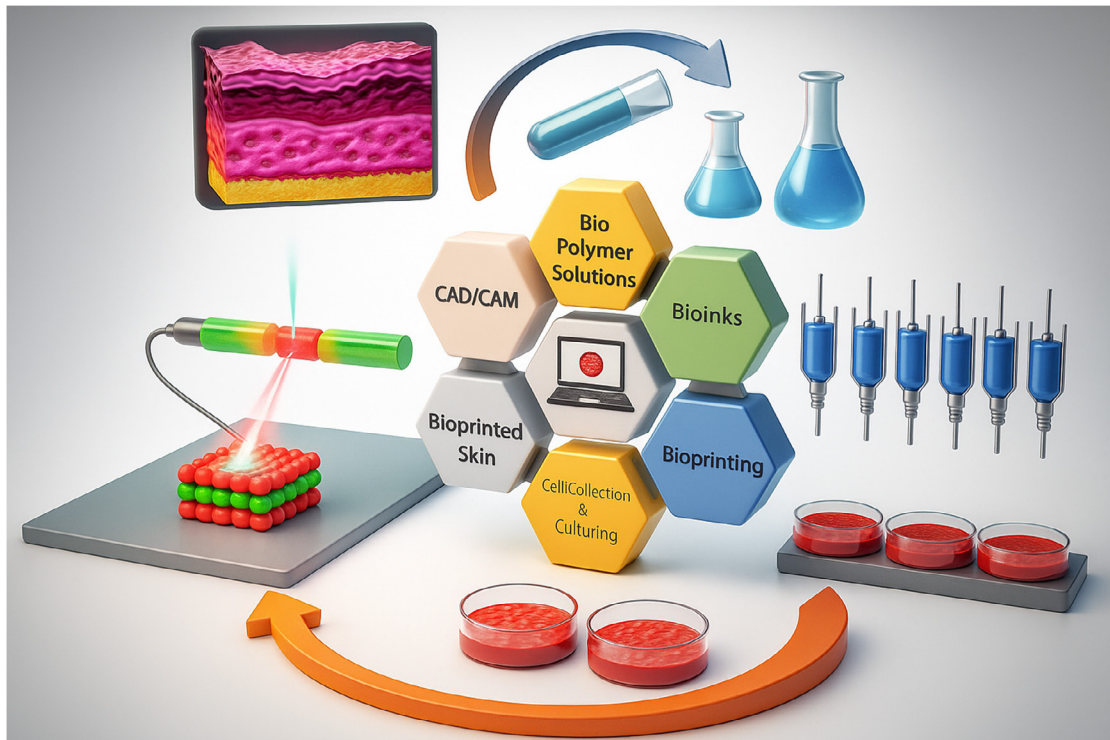


Fig. 1. Schematic representation of the generalized 3d bioprinting workflow.

[7]. The fundamental components of 3D printing consist of a printer, ink, and image files, which, along with the software components, define the desired structure for the user. In this article, various 3D printing methods and their capabilities are first reviewed, followed by a discussion on the importance of geometric infill. Subsequently, bioinks are introduced, with a particular focus on the examination of hydrogels [15].

TYPES OF 3D PRINTING METHODS

Today, there are different methods for this purpose, and each method requires inks with mechanical and physical properties tailored to it. The most important characteristics are summarized in (Figure 1) [16, 17]. Figure 1 illustrates the fundamental additive manufacturing principle underlying tissue engineering applications. The process involves the sequential layer-by-layer deposition of specialized biological inks (bioinks), guided by digital design files (e.g., CAD models derived from medical imaging), utilizing precise hardware systems (printers). Key stages include the conversion of a digital 3D model into machine instructions (slicing), the controlled extrusion,

jetting, or laser-assisted deposition of cell-laden or scaffold materials, and the formation of complex 3D structures through geometric infill patterns. This core methodology enables the fabrication of intricate, customized tissue constructs with defined architectures for biomedical research and regenerative medicine. From a hardware perspective, there are various methods of 3D printing, each differing in their ink distribution system (Figure 2). Ink distribution systems have evolved over time. Among the methods used for printing, stereolithography and molten modeling, despite their use in various industries, are not considered suitable methods for printing cellular structures due to their exposure to harmful radiation, solvent use, and high temperatures. Inkjet, extrusion, and laser-based printing are considered the three main technologies for bio-printing. These methods have the capability of shaping high-cell-density biological structures, each with its own specific strengths and weaknesses. The choice of the appropriate method is made based on factors such as cost, resolution capability, gelation speed, desired number of layers, cell viability, and other considerations [18, 19].

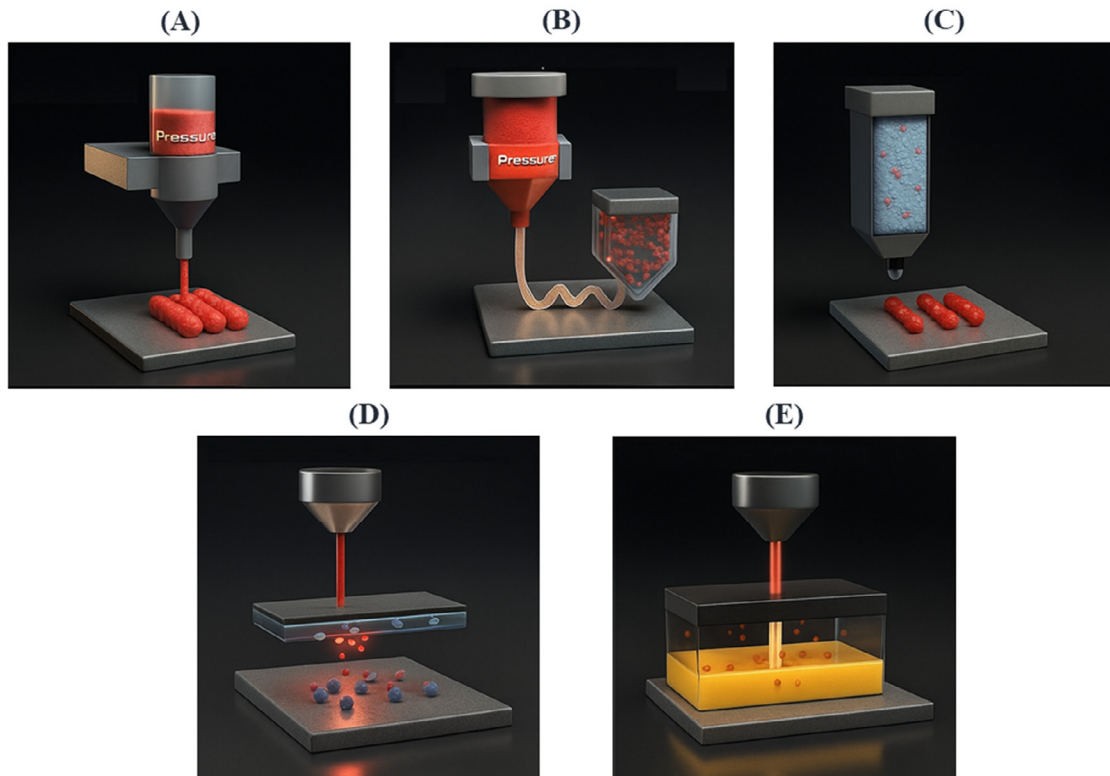


Fig. 2. Bioprinting-compatible techniques: (A) extrusion and co-axial extrusion, (B) fused deposition modelling, (C) inkjet bioprinting, (D) laser assisted bioprinting, and (E) stereolithography.

Laser-based bioprinting

Laser-based bioprinting is illustrated in (Figure 2). In this method, cells are initially trypsinized, dispersed, and subsequently suspended in a medium, such as a hydrogel. This mixture is spread onto a glass slide containing a light-absorbing coating usually made of gold or titanium. The receiving layer is positioned parallel to the first layer and placed slightly below it by a few microns to a few millimeters. Laser pulses are directed onto the absorbing layer and selectively evaporate it locally. After generating significant gas pressure due to evaporation, cellular contents are propelled towards the receiving layer [20]. It should be noted that biomaterials with high viscosity are not easily transferable in droplet form, and rapid flow formation facilitates the transfer process (Figure 3) [21]. This method's role in bioprinting lies in designing intricate scaffolds, and due to its precise layering and cell alignment capabilities, it has led to numerous studies in stem cell differentiation. Laser bioprinting, like inkjet bioprinting, is a non-contact method. Thus, there is no need for applying high pressures commonly seen in contact-based

methods. Therefore, it is considered an effective method for creating cellular patterns and scaffold-free cell culture [22].

Extrusion bioprinting

Extrusion bioprinting, also known as direct ink writing, is a widely used method in additive manufacturing based on extrusion. In this method, a liquid phase of small nozzles is distributed at a controlled flow rate and deposited layer by layer along defined patterns. The ink used in this method is distributed either mechanically (via a screw or piston) or pneumatically (through compressed gas or air). The use of piston and screw methods allows for better control of material flow rates. However, increased applied pressure may have a negative impact on cell viability [23]. In addition to piston pressure, the geometry of the nozzles is another factor affecting the applied pressure on the material. Tall cylindrical nozzles apply more shear stress compared to conical nozzles but may have better resolution capabilities [24]. Bioprinting inks for direct writing typically consist of resins or aqueous or organic solutions (solvents with



Fig. 3. A summary of the bioprinting stages of an organ (skin).

low boiling points such as dichloromethane or tetrahydrofuran) that rapidly evaporate after extrusion. Subsequently, a solid polymer matrix remains intact, preserving its structure [19]. Extrusion bioprinting accommodates precursor materials within a limited concentration and viscosity range while supporting diverse cell types. Furthermore, its configurational versatility and capacity for multi-material deposition enhance adaptability across applications. Consequently, this technique enables the fabrication of tissue constructs with tailored mechanical properties [23].

Inkjet bioprinting

In inkjet bioprinting, droplets of materials are ejected from the cartridge following the pressure generated by the formation and expulsion of microbubbles in the ink. The expulsion of bubbles can be achieved through thermal, piezoelectric, or electromagnetic stimuli. Thermal ink jetting is believed to have better biocompatibility because the frequencies used in piezoelectric and

electromagnetic methods can degrade the cell membrane due to their turbulence [19]. Inkjet printers are divided into two groups based on the mechanism of droplet generation: continuous inkjet printing and drop-on-demand inkjet printing. In continuous inkjet printing, there is a continuous flow of fluid from the ink, and by breaking it up, droplets with a diameter of approximately 100 μm are produced, and unused ink can be recycled. In drop-on-demand inkjet printing, droplets are produced individually, if necessary, with diameters ranging from 25 to 50 μm [19]. The printer deposits the desired material in a predefined pattern, and the ink is networked through physical or chemical means (UV light). Droplet formation by thermal means is achieved using a fluid chamber and single or multiple nozzles. In the bioprinting ink chamber, heat is generated, leading to the production of pressure pulses. Although this method is relatively more expensive due to the complexity of the process compared to other methods, inkjet technologies generally offer better performance efficiency, and besides non-living materials, droplets containing

encapsulated cells can be printed with high dimensional accuracy [18].

GEOMETRY IN 3D PRINTING

In 3D printing, the default nozzle diameter for most modern printers is typically 0.4 mm, and depending on the printer's usage, the nozzle can be replaceable. In addition to the nozzle diameter, which can affect printing speed and quality, an important consideration is the relationship between layer height and nozzle diameter [20]. In general, the layer height should not exceed 80% of the nozzle diameter. When using a standard 0.4 mm nozzle, the maximum layer height should be 0.32 mm. However, with a 0.6 mm nozzle, a layer height of up to 0.48 mm can be achieved. Another important aspect is the geometry of the nozzle. In addition to single-direction nozzles, various types with special geometries have been developed for specific designs. Two of the most important ones are discussed below [25].

THE EVOLUTION OF 3D PRINTERS' INKS

multi-material systems have been developed to design heterogeneous structures composed of multiple types of ink. The architecture of heterogeneous structures involves sequential printing of separate materials using multiple nozzles [26]. Cells are mixed with the desired precursor material, and it is possible to print different inks simultaneously. The main drawback of this method is its limitation in using a single ink in each unit, which not only slows down the process but also makes it impossible to use it in the design of multi-material structures [27]. Moreover, switching between different series requires stopping the ink flow, precise alignment of nozzles, and restarting ink flow. 3D printing using coaxial nozzles has been reported to create structures based on core-shell filaments, which are heterogeneous and porous. With bio-printing core-shell structures, it's possible to significantly alter the mechanical properties of pure materials. For example, core-shell composite inks such as polyethylene glycol diacrylate-alginate (with polyethylene glycol diacrylate as the shell and alginate as the core) exhibit higher tensile strength and modulus compared to pure alginate. Additionally, structures printed using core-shell bioinks have been observed to facilitate shape recovery (after deformation) [28]. Furthermore, a hydrogel based on a cell-loaded extracellular matrix can be printed as the core, while the shell consists

of a hydrogel filled with protective cells [29].

BIOPRINTING

Bioprinting, utilizing common inks and necessary features for printing Bioprinting technology is a method for shaping bio-materials through precise deposition and crosslinking, enabling the 3D printing of scaffolds in a predefined, adjustable, and reproducible manner [30]. This technology is important due to its capability of three-dimensional cell cultivation compared to existing two-dimensional methods [31]. The reason for this is the possibility of loading and anchoring different cells in various spatial positions. The use of bioprinting has been reported in the fabrication of synthetic bones, cartilage, liver, skin, as well as in studies related to tumor growth, simulation of vascular networks, and differentiation of stem cells. various types of bioprinting along with the process methods are presented. The stages of bioprinting and body organs include three main steps: preprocessing, printing, and post-processing. In the preprocessing stage, the precise structure of the target organ is designed using microscopic imaging and MRI, and this information is then used as addresses for each cell component to construct tissues or recognized organs [27]. Multiple modalities, including clinical imaging, histological section analysis, mathematical modeling, and computational simulations enable characterization of anatomical structure, tissue histology, composition, and organ topology. In the post-processing stage, the printed structure is used to create functional tissues and biological structures under laboratory conditions, requiring the maintenance of cell mass viability, growth, and induction of function (differentiation). In this stage, placing the sample in a bioreactor ensures the basic needs of cells, including oxygen, pH, moisture, temperature, nutrients, and osmotic pressure, are maintained appropriately [32].(Figure 3)

BIOLOGICAL INKS

Biological inks are recognized as liquid polymer materials rich in cells, which may contain extracellular matrix components or growth factors and essential elements for cells. Some of the printed scaffolds are formed from two or more different inks, at least one of which is biological and cellular in nature [32]. (Figure 4).

Polymer and composite materials are valuable for diverse applications [33-37]. Their unique

properties, combined with low weight, significantly enhance material design and enable researchers to develop high-quality materials [38-42]. Composite structures composed of alternating layers of biological ink and plastic (e.g., dry polymer materials), where the latter acts as the main supportive and rigid column, contributing to the strength of the scaffold [43]. Heterogeneous structures are the result of printing different layers of various inks with different compositions [44]. Complex structures where various particles such as drug carriers, nanoparticles, or chemical substances are incorporated into bioinks [45]. Various materials have been used as bio-materials in the bioprinting process. Common bioinks used in bioprinting include synthetic and natural hydrophilic polymers, extracellular matrix components, microcarriers, tissue spheroids and strands, cellular aggregates, or some advanced biological linkages such as multilateral bioinks, permeable networks, nanocomposites, and hyper molecular ones. In this regard, natural hydrogels are advantageous due to their properties such as biocompatibility, gel formation, viscosity, and providing a substrate for cell culture [46].

Biological ink should generally possess printability, shape fidelity, mechanical stability, biocompatibility, insolubility in the culture environment, non-toxicity, non-immunogenicity, facilitation of cell adhesion enhancement, appropriate degradation kinetics, and be free from secondary degradation products [47]. Achieving suitable printability of a bio-ink requires a balance among all these parameters. The required properties for a bio-ink depend on the printing method and the target tissue. Inkjet printing, for instance, requires low viscosity and thermal conductivity to prevent nozzle clogging and thermal damage. An extrusion-based bioprinting can tolerate much higher viscosity but requires attention to other properties, such as shear thinning with increasing mechanical damage potential to cells [48]. The polymer concentration in a bio-ink is another crucial factor.

An appropriate balance between viscosity and scaffold modulus should be maintained to ensure that the process is carried out without adversely affecting cell viability and migration [49]. Increasing the concentration beyond the optimal range of ink can lead to undesirable effects on cell viability by preventing cell migration and proliferation. The major challenge in creating organs or tissues using

3D printing technology is achieving mechanical, chemical, and morphological properties similar to real organs and tissues. Therefore, biological inks play a crucial role in addressing these properties. They must protect cells from structural processes such as extrusion and unfavorable environments [50]. Typically, a single biological material in a bio-ink cannot provide all the mechanical and functional requirements for tissue structure production. The use of additives such as polyethylene glycol enables modulation of physical properties necessary for the structure through molecular weight alteration and direct bonding. However, synthetic polymers of this type lack biological properties for cell adhesion, proliferation, and growth. On the other hand, the use of natural and cell-compatible biomaterials such as gelatin and fibrin face limitations due to their weak mechanical properties. Therefore, combining synthetic and natural polymers has been a strategic approach that has attracted researchers' attention [51].

INK BASED ON HYDROGEL PRECURSORS

One of the most important biomaterials is hydrogels, as they contain a significant amount of water molecules and possess excellent swelling properties [52]. Hydrogels have numerous attractive features for use as bioinks. Some of these biomaterials are light-sensitive in their modified forms and have the ability to establish cross-links. Numerous review articles have been published on the application of hydrogels in bioprinting [53]. Depending on the nature of the network precursors, a bio-ink can be transformed into either a physical or chemical hydrogel. In a chemical hydrogel, gelation occurs through the formation of covalent bonds between functional groups present in the polymers with the assistance of a crosslinking agent. Whereas, the crosslinking agent in physical gels involves secondary interactions. Ideally, the gelation process should be rapid and non-toxic to cells. Physical or chemical gelation processes can be reversible or irreversible. In all cases, physical and chemical parameters such as temperature and precursor concentration affect the gelation kinetics, appearance, and final properties of the scaffold [49].

Hydrogels, besides their application in ink, are also used as the base for strands aimed at improving the printability of inks with high viscosity and low curing rates, such as Type I collagen. The ability to break the cross-links of hydrogels by applying stress resulting from the alignment of the strands,

as well as the possibility of removing them without damaging the printed structure, are among the most important features of hydrogel-based bioinks [54].

PHYSICAL GELATION

The stimuli for physical gelation can be divided into weak intermolecular and intramolecular interactions. These hydrogels are reversible (with temperature, pressure, or other stimuli), but their bonding strength is sufficient to prevent structure dissolution in an aqueous environment. Hydrogels with physical interactions are derived from natural polysaccharides, poly(vinyl alcohol), poly(ethylene glycol), poly(N-isopropylacrylamide), poly(acrylic acid), and poly(vinyl imidazole), which can be used in the bioprinting process with various compositions [55]. In physical hydrogels, there is no need for additional chemical reactants (except ions in ionic gelation). Gelation is rapid and biocompatible, which has led to a focus on utilizing physical hydrogels in bioprinting [56].

Supramolecular interactions are among the most useful interactions in the design of physical gels, and depending on the strategy and goal, various types of these interactions can be employed. In this regard, modifying chitosan polymer with poly(ethylene glycol) and crosslinking it with cyclodextrin compounds can be mentioned. The resulting polytrioxane exhibits acceptable strain tolerance for cells, and depending on the secondary network concentration, a wide range of mechanical properties is accessible [57]. Compared to chemical hydrogels, physical hydrogels exhibit higher degradation rates and inferior mechanical properties, limiting their utility in long-term scaffolding applications. Nevertheless, post-printing characterization reveals advantageous features including self-healing capability, reduced cellular shear stress, and broad compatibility with diverse 3D printing technologies—excluding photolithography, which necessitates photocrosslinking [56]. Establishing bonds through hydrogen and van der Waals interactions can suspend the structure adequately for the printing process. When detecting a specific sequence in the polymer chain is feasible, it is called self-alignment. However, when alignment occurs only by weak and non-specific bonding, aggregation takes place. Common physical hydrogels include collagen, hyaluronic acid, and gelatin [58]. Ionic gelation begins by mixing a cation with the available

anionic parts in two or more polymer chains. For example, the establishment of connections between divalent cations like Ca^{2+} and at least two units of oligosaccharides can be cited. In the first stage, cations can be dissolved in the bioink before printing, thereby increasing the viscosity of the precursor material. It's worth mentioning that, to increase viscosity, they can be mixed with sacrificial ink [44]. Upon contact between two layers of ink, cations penetrate the bioink containing network precursors, forming bonds. Additionally, the bioink precursor network can directly deposit on a printed reservoir or on bio-paper containing cations, which, upon contact, gel the bioink. It's worth noting that reservoirs are more suitable for extrusion or inkjet printing, and bio-paper is suitable for laser printing. Finally, when the printed scaffold can maintain porosity sufficiently and for a long time, it can be immersed in cations for several minutes to establish additional bonds [45].

CHEMICAL GELATION

Involving covalent bonding of network precursors, is an irreversible process. Therefore, the resulting structure will not revert to a soluble state. However, it's possible to regulate its degradation rate with external factors such as pH, enzymes, UV light, and others [59]. A threshold precursor concentration is needed to establish chemical crosslinking. It's worth noting that, with increased concentration, structural elements and optimization of the cell-polymer rate are achieved. Since cells are a source of matrix remodeling proteases, the degradation rate of hydrogels is also controllable [60]. Polymer structures often need chemical modification before bioink preparation to have suitable reactive groups for permanent gel formation. On the other hand, attention must also be paid to biocompatibility and network formation reactions. In other words, besides ensuring that all reactants, catalysts, solvents, and products are non-toxic, reaction conditions such as temperature and pH may require specialized printers, for example, a heating system and a UV lamp for curing. In this case, their biocompatibility should also be considered [56]. A combination of physical and chemical gelation is an important solution for modulating printability and mechanical properties. For instance, in an ink composed of methacrylate gelatin-alginate, a combination of covalent and ionic networks has been used to adjust ink properties and induce heterogeneous

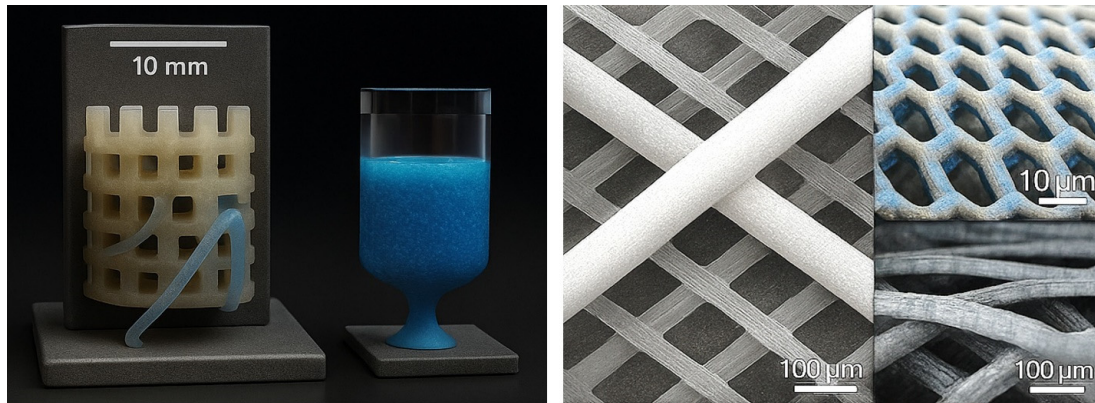


Fig. 4. Representative 3D-bioprinted constructs showing structural diversity and material innovation (Schematic illustration).

mechanical properties in the printed part. Polymer concentration and component ratios determine rheological properties, sample modulus, swelling amount, and degradation kinetics [61]. Methylcellulose represents another biomaterial of significant biotechnological relevance, necessitating both reversible and irreversible crosslinking to attain requisite mechanical properties. Grafting temperature-responsive amino groups and introducing thermosensitive hydrophobic moieties onto the polymer backbone yields a bioink that enhances mechanical performance while imparting favorable cohesive strength through partial network formation prior to injection [62].

Chemical modification of network precursors usually requires initial modification of the precursor molecules, whether they are biological molecules or synthetic polymers [63]. The most common chemical modification of network precursors involves introducing vinyl groups. Monomers based on acrylates and methacrylates are the most important carriers of vinyl groups. The second method for functionalizing polymers involves introducing thiol groups into the structure, which can contribute to crosslinking or the formation of disulfide bridges [64].

CROSSLINKING WITH LIGHT

Crosslinking can be initiated by exposure to ultraviolet (UV) or visible light in proximity to a photo initiator. While UV radiation is primarily fundamental in stereolithography printers, many bio-printers are also equipped with UV irradiation capabilities. Light-catalyzed gelation is very fast (a few seconds), and ink containing cells can be gelled immediately after exiting the printer. The precise fabrication of structures with desired

dimensional accuracy depends on two factors: the speed of gelation and the viscosity of the ink [56, 65]. The main challenges in this method include the presence of photo initiators and the potential toxicity thereof, and only a small number of them can be used at low concentrations and properly dispersed in an aqueous environment. Depending on the power and duration of irradiation, cell death and changes in cell morphology are unavoidable. Various methods have been proposed for carrying out polymerization reactions. Generally, a photo initiator is dissolved in the bio-ink or sacrificial ink, and UV curing is performed during or after printing. The two main mechanisms are photoinitiated crosslinking with chain growth and photoinitiated step-growth polymerization using two reactants, an alkene and a thiol [56].

CROSSLINKING ADHESIVES

Some hydrogels are synthesized using a crosslinker by establishing covalent interactions between two polymer chains. Various crosslinkers, such as epichlorohydrin, glutaraldehyde, and polyiodides, have been used to prepare different natural and synthetic polymer networks. Compared to dynamic bonds that are widely used, these covalent bonds are stable and irreversible under environmental conditions and the presence of stable cellular secretions. Consequently, hydrogels will have better mechanical properties and greater resistance. The main drawback of this type of bonds is the possibility of unintentional gelation in the reservoir and clogging of the dispenser [46].

NETWORK-BASED HYDROGELS

While natural hydrogels have better compatibility with cells, synthetic hydrogels demonstrate better

Table 3. Descriptive statistics for key physicochemical and biological properties of the evaluated bioinks.

Variables	Viscosity	Print Speed	Cell Viability	Mechanical Strength	Elastic Modulus	Degradation Rate	Growth Factor Release
Min	0.200	7.00	75.00	1.200	80.0	7.00	150.0
Max	1.200	15.00	95.00	2.500	200.0	30.00	220.0
Range	1.0	8.0	20.00	1.3	120.0	23.0	70.0
Mean	0.550	10.17	83.83	1.867	136.7	16.17	183.3
1st Qu.	0.325	8.25	78.50	1.575	105.0	11.00	165.0
Median	0.450	9.50	82.50	1.900	725	14.50	185.0
3st Qu.	0.650	11.50	88.75	2.150	165.0	19.50	197.5
SD	0.36	2.93	7.63	0.47	45.02	8.28	25.82
Skew	0.76	0.50	0.26	-0.08	0.11	0.51	0.04
Kurtosis	-1.07	-1.45	-1.80	-1.69	-1.80	-1.38	-1.72

processability, such as printability and shape retention [66]. To combine these two advantages, hybrids of natural and synthetic hydrogels have been developed. In these structures, the synthetic component enhances the mechanical properties of the sample, while the natural component maintains cell viability, adhesion, and cellular function by providing a cell-friendly environment similar to the extracellular matrix. Typically, in these structures, the synthetic polymer has a rigid nature, and its crosslinks are formed by establishing covalent bonds. The secondary network has a low modulus and is formed through secondary interactions, such as hydrogen bonds, ionic interactions, and coacervates. The final structure and properties of these types of structures can be adjusted by modifying the first network along with the second network [56].

STATISTICAL ANALYSIS

This study conducted a comprehensive statistical evaluation of bioink performance, employing univariate and multivariate techniques to characterize key physicochemical and biological properties. Initial descriptive statistical analysis quantified central tendency metrics, dispersion parameters, and distributional patterns for fundamental characterization parameters, including viscosity, print speed, cell viability, mechanical strength, and degradation rate. Subsequently, Pearson correlation analysis and Lasso regression modeling were employed to identify inter-variable relationships and determine the most influential predictors. Hierarchical clustering was then utilized to uncover latent groupings based on structural and functional similarities. Principal Component Analysis (PCA) and Exploratory Factor Analysis (EFA)

were further conducted to reduce dimensionality and extract latent constructs. Finally, the Technique for Order Preference by Similarity to Ideal Solution (TOPSIS) was applied to rank the bioink formulations based on multiple criteria. As shown in Table 3, the descriptive statistical analysis reflects measures of central tendency, dispersion, and distributional characteristics of the physicochemical and biological parameters. This analysis provides a comprehensive view of the dataset's statistical structure and facilitates a more accurate interpretation of material performance by identifying variability patterns and the intrinsic statistical properties of each variable. Examination of properties such as viscosity, print speed, cell viability, elastic modulus, and degradation rate reveals that many variables show approximately symmetric distributions with limited variance, while others, such as degradation rate and growth factor release, show considerable functional diversity.

The mean values of key features fell within expected ranges; for instance, viscosity was **0.55** Pa·s, cell viability averaged **83.83%**, and growth factor release was approximately **183.3** ng/mL. However, dispersion varied across variables: elastic modulus showed the greatest structural variability with a standard deviation of **45.02** MPa, whereas mechanical strength had a much narrower distribution ($SD = 0.47$ MPa), indicating greater consistency in mechanical resistance compared to structural rigidity. Analysis of skewness showed that most variables followed near-symmetric or mildly skewed distributions. Viscosity (**0.76**) and print speed (**0.50**) displayed moderate positive skewness, indicating a concentration of lower values with a few higher outliers. Mechanical strength (**-0.08**) and growth factor release (**0.04**)

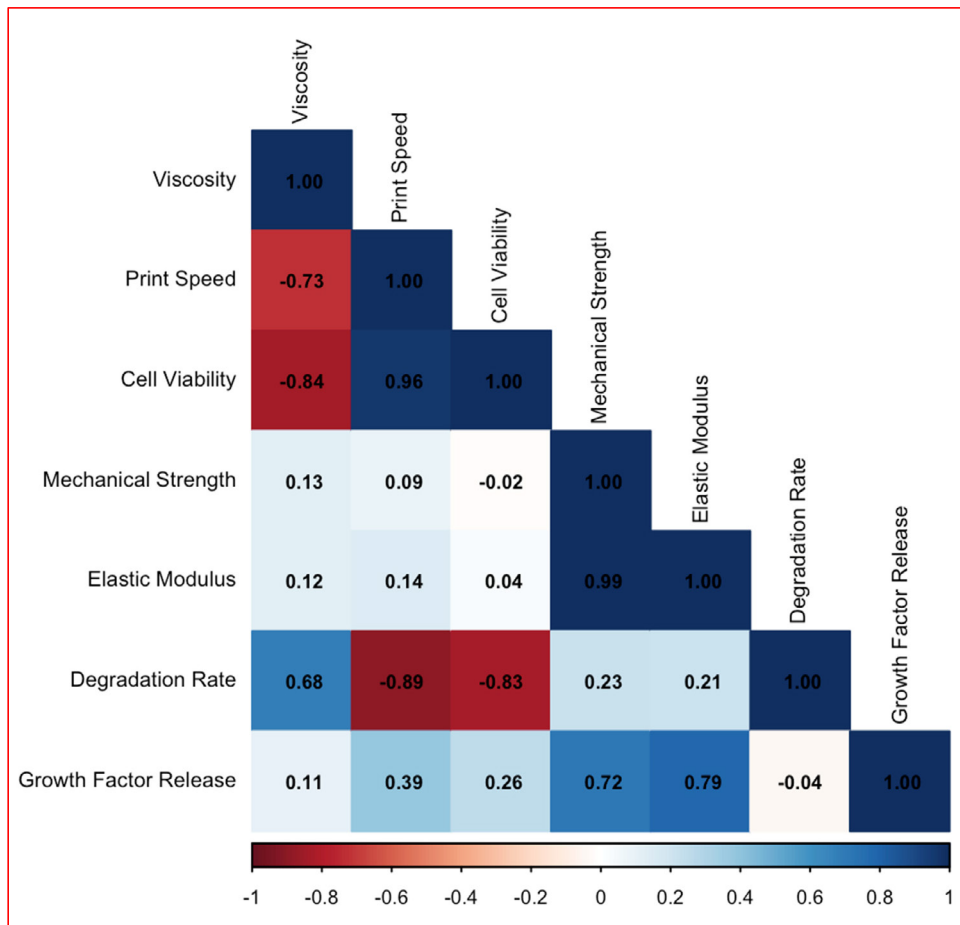


Fig. 5. Pearson correlation matrix of bioink properties.

demonstrated near-perfect symmetry.

In terms of kurtosis, all variables exhibited negative values (e.g., cell viability = -1.80), reflecting platykurtic distributions, flatter than normal curves with lighter tails. This may indicate a reduced likelihood of extreme values in certain biological properties. Additionally, the range of some parameters was substantial; degradation rate varied from 7 to 30 days (range = 23), and growth factor release spanned from 150 to 220 ng/mL (range = 70), reflecting considerable variation in bio-functional performance among the studied bioink formulations. The descriptive statistics provided a foundational understanding of the dataset, enabling more advanced multivariate analyses such as correlation, regression, and dimensionality reduction. Figure 5 presents a correlation heatmap that visualizes the pairwise relationships between key physicochemical and biological properties of bioinks. The matrix shows

distinct clusters of strongly correlated variables, as well as inverse associations that may suggest functional trade-offs in formulation design.

One of the most prominent patterns is the strong positive correlation between Cell Viability and Print Speed ($r = 0.96$), indicating that higher printing speeds may enhance cell survival, possibly by reducing shear-induced damage or exposure time. Cell Viability also exhibits a strong negative correlation with Viscosity ($r = -0.84$) and Degradation Rate ($r = -0.83$), suggesting that highly viscous or rapidly degrading formulations may adversely affect cellular outcomes. In contrast, Mechanical Strength and Elastic Modulus are highly correlated with one another ($r = 0.99$), reflecting their shared mechanical nature. These 2 variables also show moderate to strong positive correlations with Growth Factor Release ($r = 0.72$ and 0.79 , respectively), indicating that more structurally robust formulations may facilitate sustained

Table 4. Properties analysis based on Lasso regression and Pearson correlation

Features/Variables	Most Influential Predictor (Lasso)	Top Correlated Predictor	Interpretation
Cell Viability	Print Speed	Print Speed ($r = 0.96$)	Cell viability is highly dependent on print speed
Growth Factor Release	Elastic Modulus, Viscosity	Elastic Modulus ($r = 0.79$)	Release is governed by mechanical and rheological structure
Mechanical Strength	Elastic Modulus	Elastic Modulus ($r = 0.98$)	Mechanical strength is driven by elastic properties
Elastic Modulus	Mechanical Strength	Mechanical Strength ($r = 0.98$)	Elastic modulus is directly determined by structural integrity
Degradation Rate	Viscosity	Viscosity ($r = 0.88$)	Viscosity slows degradation due to higher material density
Print Speed	Degradation Rate (negative)	Degradation Rate ($r = -0.71$)	Degradation is inversely related to printing conditions
Viscosity	Degradation Rate	Degradation Rate ($r = 0.88$)	Degradation drives changes in viscosity behavior

molecular release.

Interestingly, Print Speed is negatively correlated with both Degradation Rate ($r = -0.89$) and Viscosity ($r = -0.73$), revealing that faster-printing formulations tend to be less viscous and degrade more slowly. These trade-offs evaluate the challenge of balancing competing bioink design parameters. To elucidate these relationships, Table 4 shows a multivariate analysis employing Lasso regression and Pearson correlation to quantify interdependencies among physical and biological attributes in 3D bioprinting bioinks. The results demonstrate differential influence patterns across variables. Notably, Cell Viability was primarily governed by Print Speed, which was the sole predictor retained in the Lasso model and also exhibited a strong positive linear correlation ($r = 0.96$), underscoring its pivotal role in enhancing cellular outcomes. In contrast, growth factor release was predominantly influenced by structural features such as elastic modulus and viscosity. Both predictors were selected by the Lasso model, with elastic modulus exhibiting the highest correlation with the release profile ($r = 0.79$). Mechanical characteristics such as mechanical strength and elastic modulus displayed a very strong mutual correlation ($r \approx 0.98$), reflecting their shared structural dependency. Furthermore, viscosity was identified as the most influential predictor of degradation rate, suggesting that more viscous bioinks, likely due to denser internal structures, undergo slower degradation. These correlations align with the hierarchical clustering patterns (Figure 6), further supporting the categorization of bioinks based on mechanical and rheological compatibility.

Figure 6 shows a hierarchical clustering dendrogram was constructed based on the physicochemical and biological properties of various bioink formulations. Three primary clusters can be distinguished in the analysis. In the first cluster, Alginate Ink and Hydrogel A are joined at a linkage distance of 1.18, indicating their similar rheological characteristics, including moderate viscosity and favorable printability. Gelatin-based Ink subsequently joins this group at a distance of 2.44, forming a triad characterized by high biocompatibility and relatively soft mechanical properties. The second cluster consists of Composite Hydrogel and Hydrogel B, which are grouped at a distance of 1.97. Their close association may be attributed to structural similarities, including high mechanical strength and the presence of covalent crosslinking networks. The previously formed triad is then merged with this cluster at a higher distance of 5.29, resulting in a cohesive subcluster of five materials that share functional and structural attributes.

In contrast, Collagen Ink appears as a distinctly separate formulation, joining the rest only at a much higher linkage distance of 5.55. This clear separation is likely due to its unique characteristics, including very low viscosity, exceptionally high cell viability, and rapid degradation, making it particularly suitable for soft tissue engineering applications. The reported linkage distances highlight the functional divergence among bioinks and emphasize the importance of multi-criteria design strategies in bioink formulation and selection. The PCA presented in Table 5 and Figures 7 and 8 shows a comprehensive view of the underlying structure in the dataset, effectively

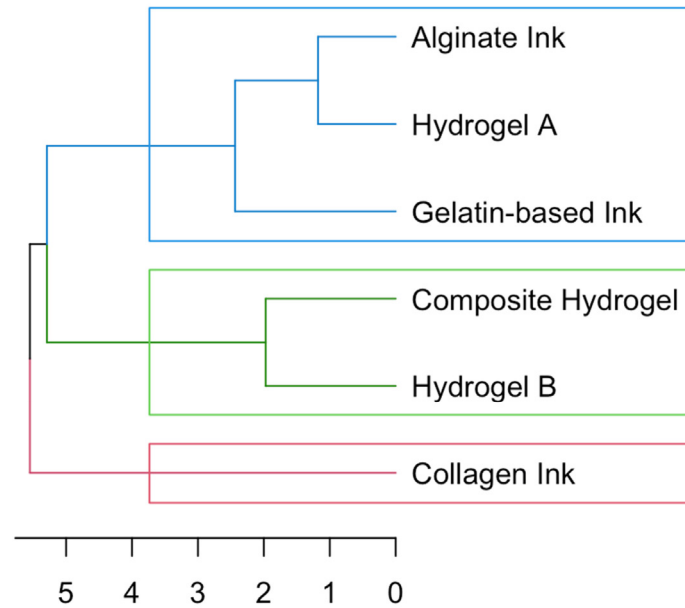


Fig. 6. Hierarchical clustering dendrogram of bioinks based on physicochemical and biological features.

Table 5. PCA Contribution

Variable	Dim.1	Dim.2	Dim.3	Dim.4	Dim.5
Viscosity	20.49	1.42	44.35	7.87	25.27
Print Speed	27.22	0.81	3.88	0.69	3.79
Cell Viability	27.35	0.03	0.08	9.80	39.20
Mechanical Strength	0.02	33.38	10.70	13.32	0.01
Elastic Modulus	0.00	35.04	5.45	2.56	3.30
Degradation Rate	23.45	1.59	9.42	41.32	9.67
Growth Factor Release	1.46	27.73	26.13	24.43	18.75

confirming the identified groupings. The number of retained principal components (Dim.1 through Dim.5) corresponds to a reduced set of orthogonal axes derived from the original seven variables via eigen decomposition of the correlation matrix. Although up to seven components are theoretically possible, only the first five were preserved, as they cumulatively accounted for the vast majority of the total variance in the data, while subsequent components contributed negligible explanatory value. Table 5 shows that Print Speed and Cell Viability contribute most significantly to the first principal component (Dim.1), with respective contributions of **27.22%** and **27.35%**, underscoring their dominant role in driving overall variability. Elastic Modulus and Mechanical Strength are the leading contributors to Dim.2

(**35.04%** and **33.38%**, respectively), reflecting their strong influence on material stiffness and load-bearing capacity. Growth Factor Release displays moderate contributions across multiple dimensions, most notably Dim.2 (**27.73%**) and Dim.3 (**26.13%**), suggesting that it captures complex, multidimensional characteristics. Meanwhile, Degradation Rate contributes substantially to Dim.1 (**23.45%**) and even more so to Dim.4 (**41.32%**), though its influence is minimal in other components. These patterns clearly demonstrate that feature importance is distributed across multiple principal components, underscoring the necessity for a detailed, multi-dimensional interpretation of the PCA results. Accordingly, for subsequent in-depth analyses, only the first two principal components (Dim.1

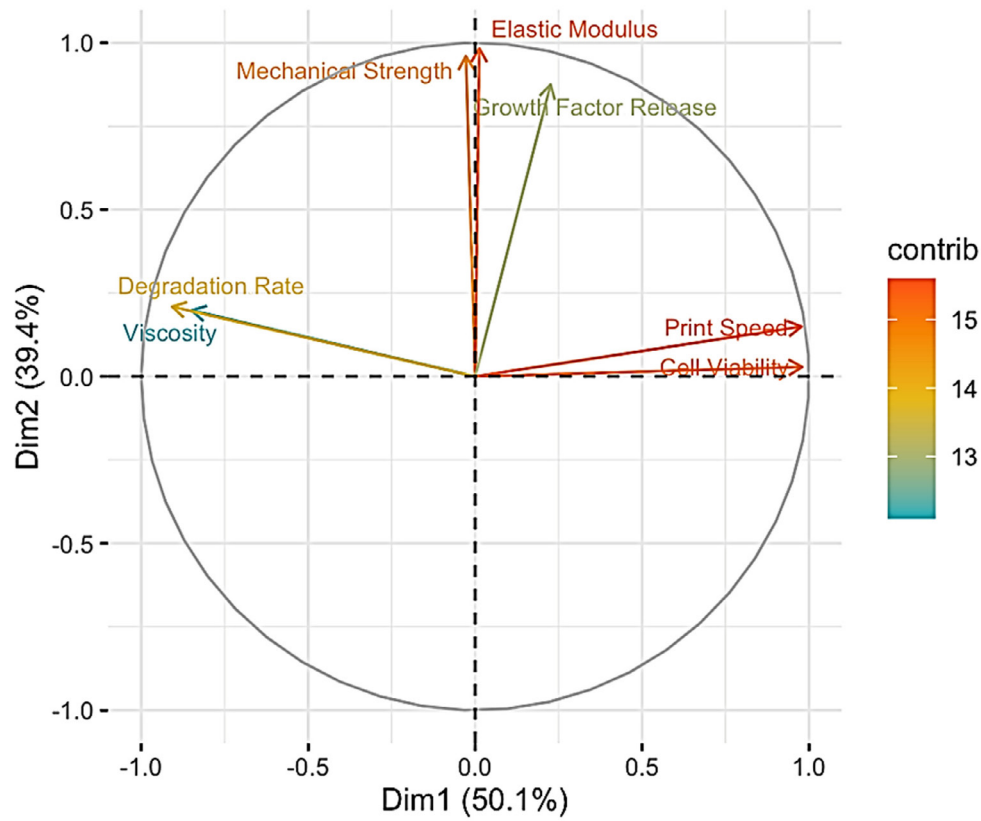


Fig. 7. PCA correlation circle illustrating the contribution of each variable to the first two principal components, with vector direction and color indicating strength and influence.

and Dim.2) were retained, as they account for the majority of total variance and represent the most meaningful structural and biological variation among the evaluated bioinks.

Figure 7 illustrates that the first two principal components (Dim1 and Dim2) capture over 90% of the total variance, effectively summarizing the multidimensional dataset. Dim1 is strongly influenced by Cell Viability and Print Speed, indicating their dominant role in bioprintability performance, while Dim2 is mainly shaped by Elastic Modulus and Mechanical Strength, reflecting material stiffness and mechanical behavior. The alignment of vectors such as Viscosity and Degradation Rate with the first principal component (Dim.1) indicates that these two features exert a similar structural influence on the data space. This parallel orientation suggests a functional linkage between rheological properties and degradation behavior in bioink formulations, potentially arising from shared underlying material mechanisms.

Figure 8 illustrates the effectiveness of PCA in distinguishing bioprinting materials based on their physicochemical and biological characteristics. Notably, Collagen Ink appears in the upper-right quadrant, clearly separated from the other materials, likely due to its superior biocompatibility and mechanical strength. In contrast, Composite Hydrogel and Hydrogel B are positioned closely together, reflecting similarities in structure and performance. Meanwhile, Hydrogel A, Alginate Ink, and Gelatin-based Ink are grouped in the lower region of the plot, suggesting comparable profiles in terms of viscosity and printability. As shown in Figure 9, the EFA was performed to explore the hidden pattern underlying the interactions between the physicochemical and biological properties of the bioinks. The results were visualized as a bipartite network, where nodes represent both the observed variables (e.g., Viscosity, Cell Viability, Elastic Modulus) and the extracted latent factors, and the edges reflect the strength and direction of the factor loadings. The analysis identified two

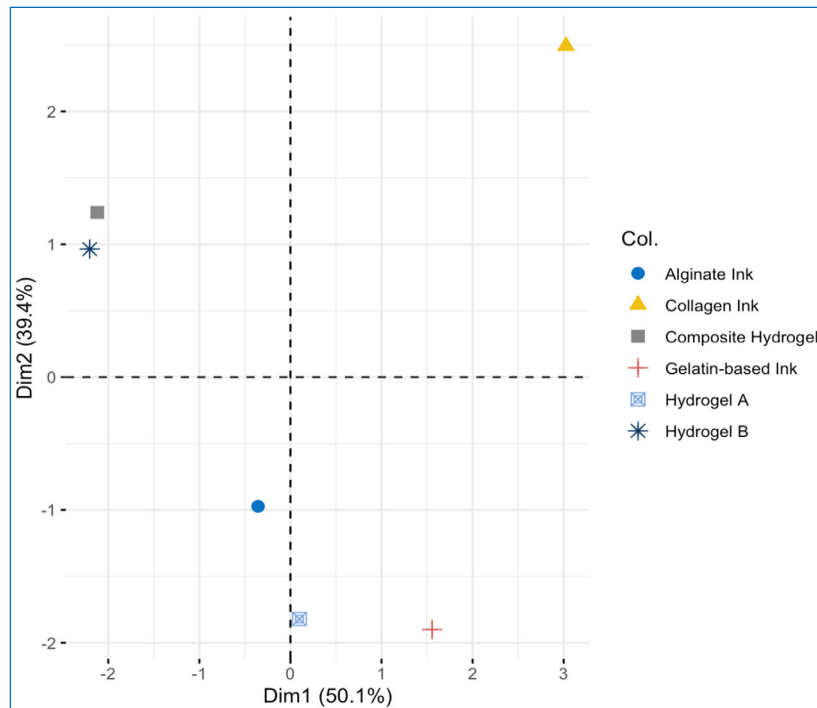


Fig. 8. PCA plot of bioprinting materials based on the first two principal components (Dim1 and Dim2).

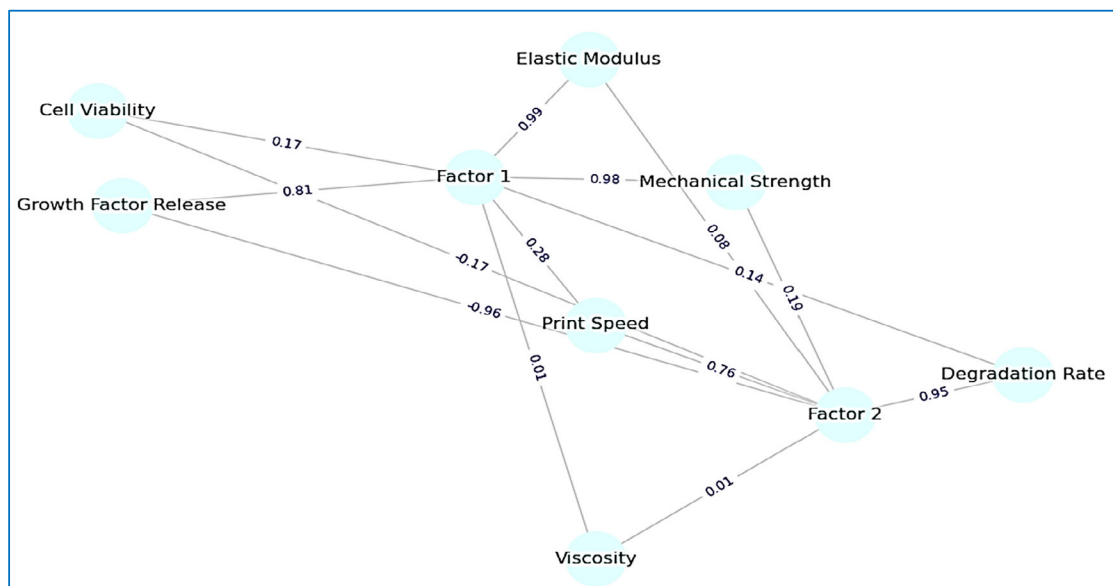


Fig. 9. Network visualization of Exploratory Factor Analysis, illustrating the relationships between observed properties and two latent factors.

latent factors. Factor 1 captures the mechanical and structural dimension, with very strong loadings on Elastic Modulus (0.99), Mechanical Strength (0.98), and Growth Factor Release (0.81), highlighting its alignment with material integrity and load-bearing capability. In contrast, Factor 2 reflects the

rheological and degradative profile of the bioinks, dominated by Degradation Rate (0.95) and Viscosity (0.76). Notably, Growth Factor Release exhibits a strong negative loading (-0.96) on this factor, suggesting a complex inverse association between structural strength and degradability or

Table 6. TOPSIS Ranking of Bioprinting Materials

Material	TOPSIS Score	Corrected Rank
Collagen Ink	1.0000	1
Composite Hydrogel	0.6692	2
Gelatin-based Ink	0.6435	3
Alginate Ink	0.5377	4
Hydrogel A	0.5271	5
Hydrogel B	0.3980	6

flow behavior. To comprehensively evaluate the performance of candidate bioinks, a multi-criteria decision-making (MCDM) approach based on the Technique for Order Preference by Similarity to Ideal Solution (TOPSIS) was employed. This evaluation was conducted using seven quantitative criteria that reflect critical rheological, mechanical, and biological characteristics of the bioinks: viscosity, print speed, cell viability, mechanical strength, elastic modulus, degradation rate, and growth factor release. As shown in the Table 6, Collagen Ink achieved the highest score 1.000, indicating its optimal performance across all evaluated criteria. It was followed by Composite Hydrogel 0.6692 and Gelatin-based Ink 0.6435, which demonstrate a well-balanced profile in terms of physicochemical and biological properties. In contrast, Hydrogel B received the lowest score 0.3980, suggesting the least suitability for bioprinting applications. This ranking provides a quantitative foundation for selecting the most appropriate materials in bioink formulation and tissue engineering design.

CONCLUSION

Following the advent of bioprinting in 2003, substantial progress has been achieved in this domain. While preclinical development of bioprinted organs advances, the complexity requisite for functional organ replacement remains incompletely characterized due to insufficient fundamental knowledge of biochemical microenvironment behaviors. Nevertheless, bioprinting constitutes a foundational technology for integrating vascular, neural, and lymphatic networks into cohesive tissue systems. Biomaterials, particularly natural hydrogels, demonstrate intrinsic immunomodulatory properties and represent promising candidates for bioprinting applications owing to their biocompatibility. It is evident that with an increase in understanding the complexities mentioned, there will be a need for platforms with intelligent features, where polymer

science plays a crucial role, especially in the realm of biomechanical exploration of printed substrates.

ACKNOWLEDGMENT

We would like to express our gratitude to Isfahan University of Medical Sciences for supporting this project under scientific code 61695 and project code 140390. We also appreciate the Ministry of Health for providing a 1% grant, which made this research possible.

FUND

This project was conducted as an open initiative under scientific code 61695 and project code 140390 at Isfahan University of Medical Sciences, receiving a 1% grant from the Ministry of Health.

CONFLICT OF INTEREST

The authors declare that they have no conflicts of interest related to this work.

REFERENCES

- Angili SN, Morovvati MR, Kardan-Halvaei M, Saber-Samandari S, Razmjooee K, Abed AM, et al. Fabrication and finite element simulation of antibacterial 3D printed Poly L-lactic acid scaffolds coated with alginate/magnesium oxide for bone tissue regeneration. *Int J Biol Macromol.* 2023;224:1152-65. <https://doi.org/10.1016/j.ijbiomac.2022.10.200>
- Esmaeili S, Shahali M, Kordjamshidi A, Torkpoor Z, Namdari F, Saber-Samandari S, et al. An artificial blood vessel fabricated by 3D printing for pharmaceutical application. *Nanomed J.* 2019;6(2):183-94.
- Iranmanesh P, Ehsani A, Khademi A, Asefnejad A, Shahriari S, Soleimani M, et al. Application of 3D bioprinters for dental pulp regeneration and tissue engineering (porous architecture). *Transp Porous Media.* 2022;142:265-93. <https://doi.org/10.1007/s11242-021-01618-x>
- Karbasian M, Eftekhari SA, Kolamroudi MK, Moghadas BK, Nasri P, Jasemi A, et al. Therapy with new generation of biodegradable and bioconjugate 3D printed artificial gastrointestinal lumen. *Iran J Basic Med Sci.* 2021;24(3):391.
- Kardan-Halvaei M, Morovvati M, Angili SN, Saber-Samandari S, Razmjooee K, Toghraie D, et al. Fabrication of 3D-printed hydroxyapatite using freeze-drying method

- for bone regeneration: RVE and finite element simulation analysis. *J Mater Res Technol.* 2023;24:8682-92. <https://doi.org/10.1016/j.jmrt.2023.05.099>
6. Karimi M, Asefnejad A, Aflaki D, Surendar A, Baharifar H, Saber-Samandari S, et al. Fabrication of shapeless scaffolds reinforced with baghdadite-magnetite nanoparticles using a 3D printer and freeze-drying technique. *J Mater Res Technol.* 2021;14:3070-9. <https://doi.org/10.1016/j.jmrt.2021.08.084>
 7. Lee JY, An J, Chua CK. Fundamentals and applications of 3D printing for novel materials. *Appl Mater Today.* 2017;7:120-33. <https://doi.org/10.1016/j.apmt.2017.02.004>
 8. Moarrefzadeh A, Morovvati MR, Angili SN, Smaism GF, Khandan A, Toghraie D. Fabrication and finite element simulation of 3D printed poly L-lactic acid scaffolds coated with alginate/carbon nanotubes for bone engineering applications. *Int J Biol Macromol.* 2023;224:1496-1508. <https://doi.org/10.1016/j.ijbiomac.2022.10.238>
 9. Sahmani S, Khandan A, Saber-Samandari S, Aghdam M. Vibrations of beam-type implants made of 3D printed bredigite-magnetite bio-nanocomposite scaffolds under axial compression: Application, communication and simulation. *Ceram Int.* 2018;44(10):11282-91. <https://doi.org/10.1016/j.ceramint.2018.03.173>
 10. Sahmani S, Khandan A, Saber-Samandari S, Esmaeili S, Aghdam MM. Fabrication and resonance simulation of 3D-printed biocomposite mesoporous implants with different periodic cellular topologies. *Bioprinting.* 2021;22:e00138. <https://doi.org/10.1016/j.bprint.2021.e00138>
 11. Salimi K, Eghbali S, Jasemi A, Shokrani F, Froushani R, Joneidi Yekta H, Latifi M, et al. An artificial soft tissue made of nano-alginate polymer using bioxfab 3D bioprinter for treatment of injuries. *Nanochem Res.* 2020;5(2):120-7.
 12. Yadav R, Naebe M, Wang X, Kandasubramanian B. Review on 3D prototyping of damage tolerant interdigitating brick arrays of nacre. *Ind Eng Chem Res.* 2017;56(37):10516-25. <https://doi.org/10.1021/acs.iecr.7b01679>
 13. Savvides L. Approaching 3D Printing. In: *3D Printing Cultures, Politics and Hackerspaces.* Emerald Publishing Limited; 2021. p. 1-27. <https://doi.org/10.1108/978-1-80071-665-020211003>
 14. MacDonald E, Wicker R. Multiprocess 3D printing for increasing component functionality. *Science.* 2016;353(6307):aaf2093. <https://doi.org/10.1126/science.aaf2093>
 15. Jandyal A, Chaturvedi I, Wazir I, Raina A, Haq MIU. 3D printing-A review of processes, materials and applications in industry 4.0. *Sustain Oper Comput.* 2022;3:33-42. <https://doi.org/10.1016/j.susoc.2021.09.004>
 16. Ozbolat IT, Moncal KK, Gudapati H. Evaluation of bioprinter technologies. *Addit Manuf.* 2017;13:179-200. <https://doi.org/10.1016/j.addma.2016.10.003>
 17. Tetsuka H, Shin SR. Materials and technical innovations in 3D printing in biomedical applications. *J Mater Chem B.* 2020;8(15):2930-50. <https://doi.org/10.1039/D0TB00034E>
 18. Buwalda SJ, Boere KW, Dijkstra PJ, Feijen J, Vermonden T, Hennink WE. Hydrogels in a historical perspective: From simple networks to smart materials. *J Control Release.* 2014;190:254-73. <https://doi.org/10.1016/j.jconrel.2014.03.052>
 19. Guvendiren M, Molde J, Soares RM, Kohn J. Designing biomaterials for 3D printing. *ACS Biomater Sci Eng.* 2016;2(10):1679-93. <https://doi.org/10.1021/acsbomaterials.6b00121>
 20. Hospodiuk M, Dey M, Sosnoski D, Ozbolat IT. The bioink: A comprehensive review on bioprintable materials. *Biotechnol Adv.* 2017;35(2):217-39. <https://doi.org/10.1016/j.biotechadv.2016.12.006>
 21. Koch L, Gruene M, Unger C, Chichkov B. Laser assisted cell printing. *Curr Pharm Biotechnol.* 2013;14(1):91-7. <https://doi.org/10.2174/1389201011314010012>
 22. Jian H, Wang M, Wang S, Wang A, Bai S. 3D bioprinting for cell culture and tissue fabrication. *Bio-Des Manuf.* 2018;1(1):45-61. <https://doi.org/10.1007/s42242-018-0006-1>
 23. Chimene D, Lennox KK, Kaunas RR, Gaharwar AK. Advanced bioinks for 3D printing: a materials science perspective. *Ann Biomed Eng.* 2016;44(6):2090-102. <https://doi.org/10.1007/s10439-016-1638-y>
 24. Bedell ML, Navara AM, Du Y, Zhang S, Mikos AG. Polymeric systems for bioprinting. *Chem Rev.* 2020;120(19):10744-792. <https://doi.org/10.1021/acs.chemrev.9b00834>
 25. Rahim TNAT, Abdullah AM, Akil HM. Recent developments in fused deposition modeling-based 3D printing of polymers and their composites. *Polym Rev.* 2019;59(4):589-624. <https://doi.org/10.1080/15583724.2019.1597883>
 26. Rafiee M, Farahani RD, Therriault D. Multi-material 3D and 4D printing: a survey. *Adv Sci.* 2020;7(12):1902307. <https://doi.org/10.1002/adv.201902307>
 27. Agarwal S, Saha S, Balla VK, Pal A, Barui A, Bodhak S. Current developments in 3D bioprinting for tissue and organ regeneration-a review. *Front Mech Eng.* 2020;6:589171. <https://doi.org/10.3389/fmech.2020.589171>
 28. Rupp H, Binder WH. 3D Printing of Core-Shell Capsule Composites for Post-Reactive and Damage Sensing Applications. *Adv Mater Technol.* 2020;5(8):2000509. <https://doi.org/10.1002/admt.202000509>
 29. Gu Z, Fu J, Lin H, He Y. Development of 3D bioprinting: From printing methods to biomedical applications. *Asian J Pharm Sci.* 2020;15(5):529-57. <https://doi.org/10.1016/j.ajps.2019.11.003>
 30. Sharma Y, Shankar V. Technologies for the fabrication of crosslinked polysaccharide-based hydrogels and its role in microbial three-dimensional bioprinting-A review. *Int J Biol Macromol.* 2023;126:194. <https://doi.org/10.1016/j.ijbiomac.2023.126194>
 31. Agrawal G, Ramesh A, Aishwarya P, Sally J, Ravi M. Devices and techniques used to obtain and analyze three-dimensional cell cultures. *Biotechnol Prog.* 2021;37(3):e3126. <https://doi.org/10.1002/btpr.3126>
 32. Augustine R. Skin bioprinting: a novel approach for creating artificial skin from synthetic and natural building blocks. *Prog Biomater.* 2018;7(2):77-92. <https://doi.org/10.1007/s40204-018-0087-0>
 33. Alimirzaei S, Barbaz-Isfahani R, Khodaei A, Najafabadi MA, Sadighi M. Investigating the flexural behavior of nanomodified multi-delaminated composites using acoustic emission technique. *Ultrasonics.* 2024;138:107249. <https://doi.org/10.1016/j.ultras.2024.107249>
 34. Barbaz Isfahani R, Shahbaz A, Khademi A, Iranmanesh P, Khandan A, Sheikhabaei E. Mechanical and Chemical Behaviour of Nanoparticles in Multicomponent Dressings: Promoting Wound Healing with Novel Materials,

- Intelligent Monitoring, and Enhanced Healing Outcomes. *Nanochem Res.* 2025. [Articles in Press]
35. Barbaz-Isfahani R, Dadras H, Taherzadeh-Fard A, Zarezadeh-Mehrzi MA, Saber-Samandari S, Salehi M, et al. Synergistic effects of incorporating various types of nanoparticles on tensile, flexural, and quasi-static behaviors of GFRP composites. *Fibers Polym.* 2022;23(7):2003-16. <https://doi.org/10.1007/s12221-022-4283-0>
 36. Dadras H, Barbaz-Isfahani R, Saber-Samandari S, Salehi M. Experimental and multi-scale finite element modeling for evaluating healing efficiency of electro-sprayed microcapsule based glass fiber-reinforced polymer composites. *Polym Compos.* 2022;43(9):5929-45. <https://doi.org/10.1002/pc.26850>
 37. Rahmani F, Barbaz-Isfahani R, Saber-Samandari S, Salehi M. Effect of corrosive environment on mechanical properties of polymer-based nanocomposite: analytical and experimental study. *Mater Today Commun.* 2023;36:106544. <https://doi.org/10.1016/j.mtcomm.2023.106544>
 38. Barbaz-Isfahani R, Dadras H, Saber-Samandari S, Taherzadeh-Fard A, Liaghat G. A comprehensive investigation of the low-velocity impact response of enhanced GFRP composites with single and hybrid loading of various types of nanoparticles. *Heliyon.* 2023;9(3). <https://doi.org/10.1016/j.heliyon.2023.e15930>
 39. Barbaz-Isfahani R, Khalvandi A, Tran TMN, Kamarian S, Saber-Samandari S, Song JI. Synergistic effects of egg shell powder and halloysite clay nanotubes on the thermal and mechanical properties of abaca/polypropylene composites. *Ind Crops Prod.* 2023;205:117498. <https://doi.org/10.1016/j.indcrop.2023.117498>
 40. Dadras H, Teimouri A, Barbaz-Isfahani R, Saber-Samandari S. Indentation, finite element modeling and artificial neural network studies on mechanical behavior of GFRP composites in an acidic environment. *J Mater Res Technol.* 2023;24:5042-58. <https://doi.org/10.1016/j.jmrt.2023.04.146>
 41. Khalvandi A, Kamarian S, Barbaz-Isfahani R, Saber-Samandari S, Song JI. On the flammability and mechanical responses of abaca-reinforced composites: a machine learning-oriented approach. *Smart Sci.* 2025;13(1):60-76. <https://doi.org/10.1080/23080477.2024.2427441>
 42. Rahmani F, Barbaz-Isfahani R, Saber-Samandari S, Salehi M. Experimental and analytical investigation on forced and free vibration of sandwich structures with reinforced composite faces in an acidic environment. *Heliyon.* 2023;9(3). <https://doi.org/10.1016/j.heliyon.2023.e20864>
 43. Gibson RF. A review of recent research on mechanics of multifunctional composite materials and structures. *Compos Struct.* 2010;92(12):2793-810. <https://doi.org/10.1016/j.compstruct.2010.05.003>
 44. Kokkinis D, Schaffner M, Studart AR. Multimaterial magnetically assisted 3D printing of composite materials. *Nat Commun.* 2015;6:8643. <https://doi.org/10.1038/ncomms9643>
 45. Valot L, Martinez J, Mehdi A, Subra G. Chemical insights into bioinks for 3D printing. *Chem Soc Rev.* 2019;48(15):4049-86. <https://doi.org/10.1039/C7CS00718C>
 46. Whitford WG, Hoying JB. A bioink by any other name: terms, concepts and constructions related to 3D bioprinting. *Future Sci.* 2016:FSO133. <https://doi.org/10.4155/fsoa-2016-0044>
 47. Kharkar PM, Kiick KL, Kloxin AM. Designing degradable hydrogels for orthogonal control of cell microenvironments. *Chem Soc Rev.* 2013;42(17):7335-72. <https://doi.org/10.1039/C3CS60040H>
 48. Akhtar MF, Hanif M, Ranjha NM. Methods of synthesis of hydrogels... A review. *Saudi Pharm J.* 2016;24(5):554-9. <https://doi.org/10.1016/j.jsps.2015.03.022>
 49. Gungor-Ozkerim PS, Inci I, Zhang YS, Khademhosseini A, Dokmeci MR. Bioinks for 3D bioprinting: an overview. *Biomater Sci.* 2018;6(5):915-46. <https://doi.org/10.1039/C7BM00765E>
 50. Donderwinkel I, Van Hest JC, Cameron NR. Bio-inks for 3D bioprinting: recent advances and future prospects. *Polym Chem.* 2017;8(30):4451-71. <https://doi.org/10.1039/C7PY00826K>
 51. Fedorovich NE, De Wijn JR, Verbout AJ, Alblas J, Dhert WJ. Three-dimensional fiber deposition of cell-laden, viable, patterned constructs for bone tissue printing. *Tissue Eng Part A.* 2008;14(1):127-33. <https://doi.org/10.1089/ten.a.2007.0158>
 52. Ngo TD, Kashani A, Imbalzano G, Nguyen KT, Hui D. Additive manufacturing (3D printing): A review of materials, methods, applications and challenges. *Compos Part B Eng.* 2018;143:172-96. <https://doi.org/10.1016/j.compositesb.2018.02.012>
 53. Mota C, Camarero-Espinosa S, Baker MB, Wieringa P, Moroni L. Bioprinting: from tissue and organ development to in vitro models. *Chem Rev.* 2020;120(19):10547-107. <https://doi.org/10.1021/acs.chemrev.9b00789>
 54. Tan EY, Suntornmond R, Yeong WY. High-resolution novel indirect bioprinting of low-viscosity cell-laden hydrogels via model-support bioink interaction. *3D Print Addit Manuf.* 2021;8(2):69-78. <https://doi.org/10.1089/3dp.2020.0153>
 55. Gholamali I. Stimuli-responsive polysaccharide hydrogels for biomedical applications: a review. *Regen Eng Transl Med.* 2021;7(1):91-114. <https://doi.org/10.1007/s40883-019-00134-1>
 56. Akkineni AR, Ahlfeld T, Lode A, Gelinsky M. A versatile method for combining different biopolymers in a core/shell fashion by 3D plotting to achieve mechanically robust constructs. *Biofabrication.* 2016;8(4):045001. <https://doi.org/10.1088/1758-5090/8/4/045001>
 57. Hu T, Cui X, Zhu M, Wu M, Tian Y, Yao B, et al. 3D-printable supramolecular hydrogels with shear-thinning property: Fabricating strength tunable bioink via dual crosslinking. *Bioact Mater.* 2020;5(4):808-18. <https://doi.org/10.1016/j.bioactmat.2020.06.001>
 58. Hoch E, Hirth T, Tovar GE, Borchers K. Chemical tailoring of gelatin to adjust its chemical and physical properties for functional bioprinting. *J Mater Chem B.* 2013;1(42):5675-85. <https://doi.org/10.1039/c3tb20745e>
 59. Andreu A, Lee H, Kang J, Yoon YJ. Self-Healing Materials for 3D Printing. *Adv Funct Mater.* 2024;2315046. <https://doi.org/10.1002/adfm.202315046>
 60. Bijalwan V, Rana S, Yun GJ, Singh KP, Jamil M, Schlägl S. 3D Printing of Covalent Adaptable Networks: Overview, Applications and Future Prospects. *Polym Rev.* 2024;64(1):36-79. <https://doi.org/10.1080/15583724.2023.2227692>
 61. Aldana AA, Valente F, Dillely R, Doyle B. Development of 3D bioprinted GelMA-alginate hydrogels with tunable mechanical properties. *Bioprinting.* 2021;21:e00105.

- <https://doi.org/10.1016/j.bprint.2020.e00105>
62. Shin JY, Yeo YH, Jeong JE, Park SA, Park WH. Dual-crosslinked methylcellulose hydrogels for 3D bioprinting applications. *Carbohydr Polym.* 2020;238:116192. <https://doi.org/10.1016/j.carbpol.2020.116192>
 63. Dufour T. From basics to frontiers: A comprehensive review of plasma-modified and plasma-synthesized polymer films. *Polymers.* 2023;15(17):3607. <https://doi.org/10.3390/polym15173607>
 64. Yu C, Schimelman J, Wang P, Miller KL, Ma X, You S, et al. Photopolymerizable biomaterials and light-based 3D printing strategies for biomedical applications. *Chem Rev.* 2020;120(19):10695-743. <https://doi.org/10.1021/acs.chemrev.9b00810>
 65. Zhang X, Jiang X, Sun C. Micro-stereolithography of polymeric and ceramic microstructures. *Sens Actuators A Phys.* 1999;77(2):149-56. [https://doi.org/10.1016/S0924-4247\(99\)00189-2](https://doi.org/10.1016/S0924-4247(99)00189-2)
 66. Fatimi A, Okoro OV, Podstawczyk D, Siminska-Stanny J, Shavandi A. Natural hydrogel-based bio-inks for 3D bioprinting in tissue engineering: a review. *Gels.* 2022;8(3):179. <https://doi.org/10.3390/gels8030179>